



Numerical Simulation of the Impact of Ice Accumulation on a Composite Wind Turbine Blades located in a Cold Climate

Oumnia Lagdani, Mostapha Tarfaoui, Mourad Nachtane, M. Trihi, H. Laaouidi

► To cite this version:

Oumnia Lagdani, Mostapha Tarfaoui, Mourad Nachtane, M. Trihi, H. Laaouidi. Numerical Simulation of the Impact of Ice Accumulation on a Composite Wind Turbine Blades located in a Cold Climate. 3rd International Conference of Computer Science and Renewable Energies, ICCSRE 2020, Dec 2020, Agadir, Morocco. pp.01052, 10.1051/e3sconf/202122901052 . hal-03151958

HAL Id: hal-03151958

<https://ensta-bretagne.hal.science/hal-03151958>

Submitted on 25 Feb 2021

HAL is a multi-disciplinary open access archive for the deposit and dissemination of scientific research documents, whether they are published or not. The documents may come from teaching and research institutions in France or abroad, or from public or private research centers.

L'archive ouverte pluridisciplinaire **HAL**, est destinée au dépôt et à la diffusion de documents scientifiques de niveau recherche, publiés ou non, émanant des établissements d'enseignement et de recherche français ou étrangers, des laboratoires publics ou privés.

Numerical Simulation of the Impact of Ice Accumulation on a Composite Wind Turbine Blades located in a Cold Climate

O. Lagdani^{1*}, M. Tarfaoui², M. Nachtane³, M. Trihi¹ and H. Laaouidi¹

¹Laboratory for Renewable Energy and Dynamic Systems, FSAC - UH2C, Morocco

²ENSTA Bretagne, IRDL UMR CNRS 6027, F-29200 Brest, France

³University of Bordeaux, CNRS, Arts et Metiers Institute of Technology, Bordeaux INP, INRAE, I2M Bordeaux, F-33400 Talence, France

Oumnialagdani@gmail.com, mostapha.tarfaoui@ensta-bretagne.fr

Keywords: Cold climate, Composite wind turbine blade, Ice Accretion, Numerical analysis, Hashin criterion, Finite element analysis.

Abstract: The blades of wind turbines placed in cold climate regions are exposed to the risk of icing phenomena which impact their lifetimes. This paper proposes a numerical model to simulate 50 mm ice thickness localized on the tip side of a horizontal wind turbine blade, and to study its mechanical behavior. The wind turbine blade was modeled with the finite element method (FEM) in ABAQUS software taking into account aerodynamic, centrifugal and inertial loads under the conditions of service of the blade. Numerical tests have evaluated the behavior of different composite materials and compared with each other. Damage mode based on the Hashin criteria was defined. Carbon fibers were considered to be the most rigid material which results in thinner, stiffer and lighter blades.

1 INTRODUCTION

Offshore wind energy is among the most advanced and modern technologies currently available to provide clean energy, due to the high average wind speeds that regularly blow over the oceans [1]. Cold regions are considered as the best areas for wind energy, which is therefore a dynamic and growing sector. However, one of the problems encountered in these zones is the accumulation of ice on the surface of wind turbines. The wind energy loss depends mainly on the quantity of ice accreted on the blades [2]. The icing process results in a considerable degradation of energy due to performance deterioration caused by excessive vibration problems of the rotor. It is also necessary to note the severe dangers caused by ice projection from the blade producing unpleasant noise [3].

Composite materials such as Carbon or Glass fibers are used as alternative materials to steel because of their significant potential advantages in offshore applications and their attractive properties [4]. The formation of ice on several parts of the wind turbine using these materials will affect their mechanical properties.

In the present paper, a numerical analysis has been performed to study the mechanical behavior and the influence of ice formation on offshore wind turbine blades. The analysis is presented using ABAQUS software based on the Finite Element Method (FEM) taking into account different aerodynamic loads and using several materials.

2

STRUCTURAL PERFORMANCE ANALYSIS

2.1 Structural configuration of the blade

The system adopted for this study is composed of a rigid three-bladed offshore wind turbine. The blade is manufactured to produce 5 MW of a maximum power using NACA 4412 profile with well-known aerodynamic characteristics [5]-[6].

The parameters of the model used are summarized in Table 1.

Table 1: Specifications of the wind turbine blade

Airfoil	NACA 4412
Length of the blade (m)	48
Number of blades	3
Maximum chord (mm)	3932
Position twists maximum (mm)	R9000
Fluid speed upstream of the blade (m/s)	25
Angular velocity (rpm)	15.7

Rotor blade consists of several parts combined together to form the aerofoil shape, in order to provide a greater number of possible combinations of the materials employed as required, Figure 1[7]-[8].

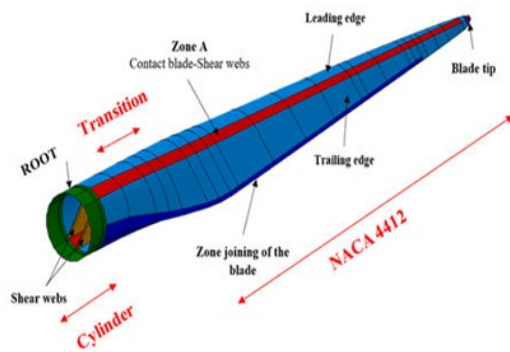


Figure 1: Division of the blade structure

2.2 Mechanical properties description

The majority of the wind turbines blades are manufactured by using composite materials because of their interesting properties and excellent mass/durability relations[9]-[10]. Carbon and Glass fibers have been chosen to evaluate the behavior of the blade. Their characteristic properties are summarized in Table 2.

Table2: Mechanical properties of the materials employed in the analysis of the wind turbine blade

Engineer ing const ants	Material Properties	Carbon-epoxy [11]	Glass-polyester [12]
	ρ (kg/m ³)	1600	1960
	E_1 (GPa)	147	48.16
	E_2 (GPa) = E_3 (GPa)	10.3	11.210
	$\nu_{12} = \nu_{13}$	0.27	0.270
	ν_{23}	0.54	0.096
	G_{12} (GPa) = G_{13} (GPa)	7	4.420
	G_{23} (GPa)	3.7	9
	X_t (MPa)	2041	1021
	X_c (MPa)	1784	978
Strength properties			

Y_t (MPa)	58.7	29.5
Y_c (MPa)	24.78	171.8
$S_t = S_c$ (MPa)	65.6	35.3

3 HASHIN'S THEORY

Hashin's model is among the most popular criteria and widely used in composite structure applications due to its simplicity of design and ease of use[13]. The Hashin type failure criterion has been employed to predict and detect damage in composite structures. It consists of two failure mechanisms, one associated with fiber failure and the other with matrix failure, differentiating between tension and compression[14]-[15].

The four distinct modes of damage are represented as follows:

Fiber tension (HSNFTCRT), $\hat{\sigma}_{11} \geq 0$:

$$\left(\frac{\hat{\sigma}_{11}}{X_T}\right)^2 + \alpha \times \left(\frac{\hat{\sigma}_{12}}{S_{LT}}\right)^2 = f_1 \quad (1)$$

Fiber compression (HSNFCCRT), $\hat{\sigma}_{11} < 0$:

$$\left(\frac{\hat{\sigma}_{11}}{X_T}\right)^2 + \alpha \times \left(\frac{\hat{\sigma}_{12}}{S_{LT}}\right)^2 = f_1 \quad (2)$$

Matrix tension (HSNMTCRT), $\hat{\sigma}_{22} \geq 0$:

$$\left(\frac{\hat{\sigma}_{11}}{X_T}\right)^2 + \alpha \times \left(\frac{\hat{\sigma}_{12}}{S_{LT}}\right)^2 = f_1 \quad (3)$$

Matrix compression (HSNMCCRT), $\hat{\sigma}_{22} < 0$:

$$\left(\frac{\hat{\sigma}_{11}}{X_T}\right)^2 + \alpha \times \left(\frac{\hat{\sigma}_{12}}{S_{LT}}\right)^2 = f_1 \quad (4)$$

4 NUMERICAL ANALYSIS

4.1 Boundary Conditions

Figure 2 illustrates the boundary condition assigned to the blade using "Encastre" type applied at the root[16].

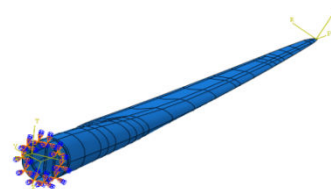


Figure 2: Encastre boundary condition

4.2 Loads

Wind turbines are subject to various loads applied to their entire structure. They are defined as aerodynamic loads that are generated by a rotor blade, and operating on it are greatly variable in intensity because of the stochastic character of the wind field. Inertia and gravitational loads are also taken into account in this study [17].

The three loads were then simultaneously applied using the ABAQUS software on a horizontal blade Figure 3, containing ice at the end of the structure as shown in the Figure 4. Table 3 provides some ice layer information used in this study.

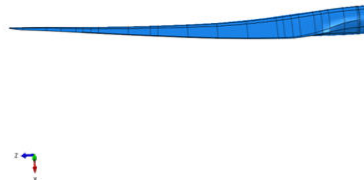


Figure 3: Position of the blade



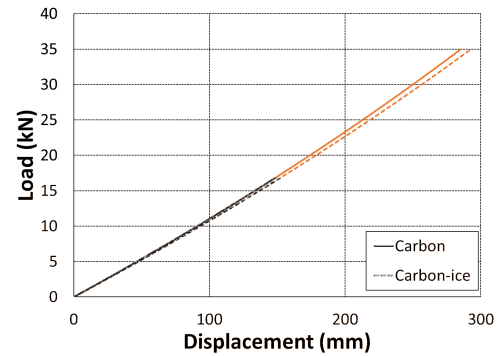
Figure 4: Iced wind turbine blade

Table 3: Ice layer information

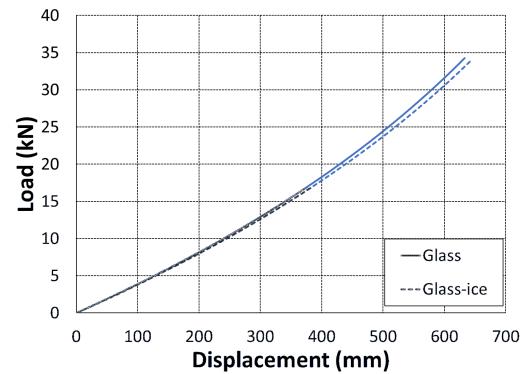
Length of ice cover (m)	Distance from rotor (m)	Thickness of ice (mm)	Mass of ice (kg)
3.21	43.031	50	0.303

5 RESULTS AND ANALYSIS

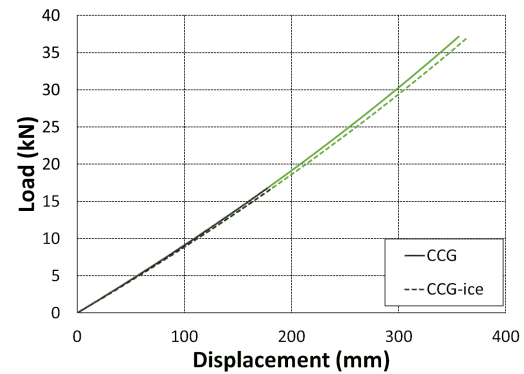
After defining and identifying the loads, our first objective is to analyze the behavior of the blade using both Carbon and Glass fibers, and then discover the effect of the hybrid Carbon-Glass located at section C of a Carbon blade, as presented before in Figure 1.



(a) Carbon



(b) Glass



(c) CGG

Figure 5: Mechanical behavior of the clean and iced composite blade, for different materials

Figure 5 shows a comparison of load-displacement curves with various composite materials. It can be seen that the clean blade always moves less when the ice is formed at its extremity. Glass fibers have a maximum displacement value of about 632.808 mm for the clean blade and increases by about 2% for the

iced one to reach a value of 645.492 mm. While the Carbon fibers have the smallest maximum displacement and a maximum force value respectively 34.968 kN and 34.900 kN for the clean and iced blade, which makes an approximate reduction of 0.195%.

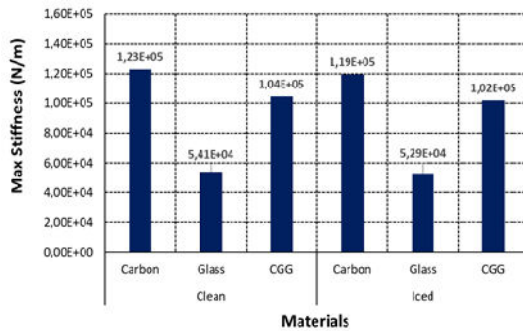


Figure 6: Maximum stiffness of the clean and iced composite blade

From Figure 6, it is clear that the maximum stiffness values vary according to the material. It is also distinguished that Carbon fibers have always the high stiffness value ($1.230 \cdot 10^5$ N/m for clean blade, and $1.194 \cdot 10^5$ N/m for iced blade) compared to other materials, which makes it the best choice for the blade design to keep it as light and as rigid as possible.

Table 4: Hashin failure data of the clean and iced composite blade

	Carbon	Glass	CGG
Clean			
HSNFCCRT	3,73E-03	7,34E-03	4,77E-03
HSNFTCRT	1,83E-02	3,98E-02	2,32E-02
HSNMCCRT	5,79E-02	3,18E-01	7,66E-02
HSNMTCRT	1,30E-01	1,00E+00	2,35E-01
Iced			
HSNFCCRT	3,98E-03	7,74E-03	4,77E-03
HSNFTCRT	1,98E-02	4,40E-02	2,32E-02
HSNMCCRT	6,25E-02	3,42E-01	7,66E-02
HSNMTCRT	1,40E-01	1,00E+00	2,35E-01

Table 4 contains the results of Hashin failure criterion of the clean and iced composite blade. A value of 1.0 was obtained for the matrix tension (HSNMTCRT) of a Glass blade, indicating that the initiation criterion was achieved.

The damage occurred at the root of the composite blade of the wind turbine due to the thickness transitions, which is highlighted in Figure 17 by the red color.

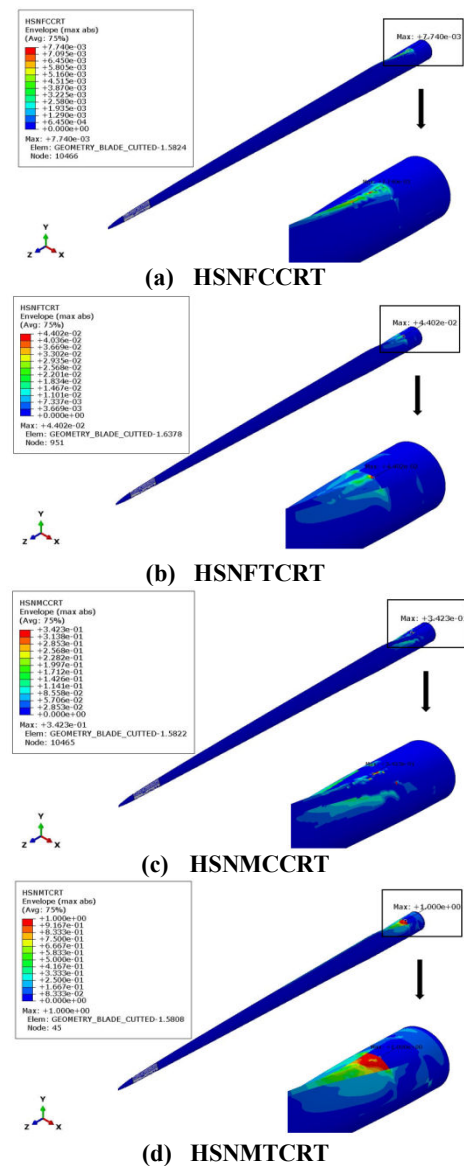


Figure 7: Hashin damage criterion for glass composite blade with 50 mm of ice

6 CONCLUSIONS

In this work, rotor performance analysis of a wind turbines placed on a horizontal position subject to icing event was performed using ABAQUS software. The blade in service was exposed to three loads at the same time with 50 mm of ice thickness located on its tip. Carbon, Glass fibers and hybrid Carbon-Glass (CGG) are the materials adopted for the conception of the blade structure. It was found that the Carbon is the strongest and most resistant

material. The root of the composite blade of the wind turbine was defined as the most susceptible region to damage and breakage. It is therefore essential to reinforce this area in order to have a stronger structure.

REFERENCES

- [1] Tarfaoui, M., rahaman shah, owaisur, &Nachtane, M. 2019. Design and optimization of composite offshore wind turbine blades. *Journal of Energy Resources Technology*.
- [2] Yirtici, O., &Tuncer, I. H. 2020. Aerodynamic Shape Optimization of Wind Turbine Blades to Reduce Power Losses due to Icing.
- [3]Wang, Q., Xiao, J., Zhang, T., Yang, J., & Shi, Y. 2020. A new wind turbine icing computational model based on Free Wake Lifting Line Model and Finite Area Method.
- [4]O'Leary, K., Pakrashi, V., &Kelliher, D. 2019. Optimization of composite material tower for offshore wind turbine structures. *Renewable Energy*.
- [5]M. Tarfaoui, J.Y. Pradillon, O.R. Shah. 2015. Numerical investigation of a large composite wind turbine with different spar profiles using finite-element method. *La Houille Blanche*, n° 5, p. 29-35
- [6]M.Nachtane, M.Tarfaoui, D.Saifaoui, A.El Moumen. Finite element analysis of composite wind turbine blade under the critical loads. *Eleven International Conference on Thermal Engineering: Theory and Applications* February 25-28, 2018, Doha, Qatar.
- [7] R.Abouchoukri. 2018. Design, Fabrication, and Operation of a Small homemade Wind Turbine Blades.
- [8] Tarfaoui, M., Nachtane, M., Khadimallah, H., &Saifaoui, D. 2017. Simulation of Mechanical Behavior and Damage of a Large Composite Wind Turbine Blade under Critical Loads. *Applied Composite Materials*, 25(2), 237–254.
- [9] M. Nachtane, M. Tarfaoui, M.Ait Mohammed, D. Saifaoui, A. El Moumen. Effects of environmental exposure on the mechanical properties of composite tidal current turbine. *Renewable Energy* 2020, 156, 1132-1145.
- [10]Nachtane, M., Tarfaoui, M., Goda, I., &Rouway, M. 2020. A review on the technologies, design considerations and numerical models of tidal current turbines. *Renewable Energy*.
- [11] M.Nachtane, M.Tarfaoui, D.Saifaoui, A.El Moumen, O.H.Hassoon, H.Benyahia. 2018. Evaluation of durability of composite materials applied to renewable marine energy: Case of ducted tidal turbine. *Energy Reports*, Volume 4, Pages 31-40.
- [12] Gemi, L. 2018. Investigation of the effect of stacking sequence on low velocity impact response and damage formation in hybrid composite pipes under internal pressure. A comparative study. *Composites Part B: Engineering*, 153, 217–232.
- [13]Gu, J., & Chen, P. 2017. Some modifications of Hashin's failure criteria for unidirectional composite materials. *Composite Structures*, 182, 143–152.
- [14] K.Kodagali., 2017. Thesis, Progressive Failure Analysis of composite Materials using the Puck Failure Criteria.
- [15] Kim Martineli Souza Gonçalves. 2015. Hashin's Failure Criteria In-Plane Stress Numerical Model Correlated to Tensile Tests. *International Journal of Engineering Research and Science & Technology*.
- [16] H. Boudounit, M. Tarfaoui, D. Saifaoui. 2019. Structural Design and Analysis of a 5MW Offshore Wind Turbine Blades Under Critical Aerodynamic Loads. *14th Congress of Mechanics* April 16-19, 2019 (Rabat, MOROCCO).
- [17]Söker, H. 2013. Loads on wind turbine blades. *Advances in Wind Turbine Blade Design and Materials*, 29–58.